ARL-RP-0536 ● SEP 2015

US Army Research Laboratory

A Molecularly Imprinted Polymer (MIP)-Coated Microbeam MEMS Sensor for Chemical Detection

by Ellen L Holthoff, Lily Li, Tobias Hiller, and Kimberly L Turner

A reprint from Proc. of SPIE Vol. 9455 94550W-1.

NOTICES

Disclaimers

The findings in this report are not to be construed as an official Department of the Army position unless so designated by other authorized documents.

Citation of manufacturer's or trade names does not constitute an official endorsement or approval of the use thereof.

Destroy this report when it is no longer needed. Do not return it to the originator.

ARL-RP-0536 ● SEP 2015

US Army Research Laboratory

A Molecularly Imprinted Polymer (MIP)-Coated Microbeam MEMS Sensor for Chemical Detection

by Ellen L Holthoff
Sensors and Electron Devices Directorate, ARL

Lily Li, Tobias Hiller, and Kimberly L Turner
Univ of California Santa Barbara, Department of Mechanical Engineering, Science Building, Room 3231 E, Santa Barbara, CA 93106

A reprint from Proc. of SPIE Vol. 9455 94550W-1.

REPORT DOCUMENTATION PAGE

Form Approved
OMB No. 0704-0188

1. REPORT DATE *(DD-MM-YYYY)*	2. REPORT TYPE	3. DATES COVERED (From - To)
Sep 2015	Reprint	

4. TITLE AND SUBTITLE

A Molecularly Imprinted Polymer (MIP)-Coated Microbeam MEMS Sensor for Chemical Detection

5a. CONTRACT NUMBER

5b. GRANT NUMBER

5c. PROGRAM ELEMENT NUMBER

6. AUTHOR(S)

Ellen L. Holthoff (1), Lily Li (2), Tobias Hiller (2), and Kimberly L. Turner (2)

5d. PROJECT NUMBER

5e. TASK NUMBER

5f. WORK UNIT NUMBER

7. PERFORMING ORGANIZATION NAME(S) AND ADDRESS(ES)

(1) US Army Research Laboratory
ATTN: RDRL-SEE-E
2800 Powder Mill Road, Adelphi, MD 20783
(2) University of California Santa Barbara, Department of Mechanical Engineering, Engineering Science Building, Room 3231 E Santa Barbara, CA 93106, Department of Mechanical Engineering, Engineering Science Building, Room 3231 E, Santa Barbara, CA 93106

8. PERFORMING ORGANIZATION REPORT NUMBER

ARL-RP-0536

9. SPONSORING/MONITORING AGENCY NAME(S) AND ADDRESS(ES)

10. SPONSOR/MONITOR'S ACRONYM(S)

11. SPONSOR/MONITOR'S REPORT NUMBER(S)

12. DISTRIBUTION/AVAILABILITY STATEMENT

Approved for public release; distribution unlimited.

13. SUPPLEMENTARY NOTES

A reprint from Proc. of SPIE Vol. 9455 94550W-1.

14. ABSTRACT

Recently, microcantilever-based technology has emerged as a viable sensing platform due to its many advantages such as small size, high sensitivity, and low cost. However, microcantilevers lack the inherent ability to selectively identify hazardous chemicals (e.g., explosives, chemical warfare agents). The key to overcoming this challenge is to functionalize the top surface of the microcantilever with a receptor material (e.g., a polymer coating) so that selective binding between the cantilever and analyte of interest takes place. Molecularly imprinted polymers (MIPs) can be utilized as artificial recognition elements for target chemical analytes of interest. Molecular imprinting involves arranging polymerizable functional monomers around a template molecule followed by polymerization and template removal. The selectivity for the target analyte is based on the spatial orientation of the binding site and covalent or noncovalent interactions between the functional monomer and the analyte. In this work, thin films of sol-gel-derived xerogels molecularly imprinted for TNT and dimethyl methylphosphonate (DMMP), a chemical warfare agent stimulant, have demonstrated selectivity and stability in combination with a fixed-fixed beam microelectromechanical systems (MEMS)-based gas sensor. The sensor was characterized by parametric bifurcation noise-based tracking.

15. SUBJECT TERMS

Molecular imprinting, microcantilever, xerogel, chemical sensor, explosives detection

16. SECURITY CLASSIFICATION OF:			17. LIMITATION OF ABSTRACT	18. NUMBER OF PAGES	19a. NAME OF RESPONSIBLE PERSON
a. REPORT	b. ABSTRACT	c. THIS PAGE			Ellen L. Holthoff
Unclassified	Unclassified	Unclassified	UU	19	19b. TELEPHONE NUMBER (Include area code) 301-394-0939

A Molecularly Imprinted Polymer (MIP)-Coated Microbeam MEMS Sensor for Chemical Detection

Ellen L. Holthoff[1], Lily Li[2], Tobias Hiller[2], and Kimberly L. Turner[2]
[1]U.S. Army Research Laboratory, RDRL-SEE-E, 2800 Powder Mill Road, Adelphi, MD 20783
[2]University of California Santa Barbara, Department of Mechanical Engineering, Engineering Science Building, Room 3231 E, Santa Barbara, CA 93106

ABSTRACT

Recently, microcantilever-based technology has emerged as a viable sensing platform due to its many advantages such as small size, high sensitivity, and low cost. However, microcantilevers lack the inherent ability to selectively identify hazardous chemicals (e.g., explosives, chemical warfare agents). The key to overcoming this challenge is to functionalize the top surface of the microcantilever with a receptor material (e.g., a polymer coating) so that selective binding between the cantilever and analyte of interest takes place. Molecularly imprinted polymers (MIPs) can be utilized as artificial recognition elements for target chemical analytes of interest. Molecular imprinting involves arranging polymerizable functional monomers around a template molecule followed by polymerization and template removal. The selectivity for the target analyte is based on the spatial orientation of the binding site and covalent or noncovalent interactions between the functional monomer and the analyte. In this work, thin films of sol-gel-derived xerogels molecularly imprinted for TNT and dimethyl methylphosphonate (DMMP), a chemical warfare agent stimulant, have demonstrated selectivity and stability in combination with a fixed-fixed beam microelectromechanical systems (MEMS)-based gas sensor. The sensor was characterized by parametric bifurcation noise-based tracking.

Keywords: Molecular imprinting, microcantilever, xerogel, chemical sensor, explosives detection

1. INTRODUCTION

Monitoring trace gases is of great importance in a wide range of applications. Rapid detection and identification of chemical warfare agents and energetic materials is a priority for Military and Homeland Defense applications. Detecting a diverse range of chemical agents requires an adaptable sensor platform capable of identifying threats before they cause harm. Research and development in hazardous-materials detection technology focuses on increasing speed, sensitivity, and selectivity, while reducing size and cost. Although the current state-of-the-art vapor detector (Joint Chemical Agent Detector (JCAD)) is lightweight, handheld, and easily attaches to a belt, it still provides added bulk to a soldier on foot patrol. Recently, microcantilever-based technology has emerged as a viable platform due to its many advantages such as small size, high sensitivity, and low cost.[1, 2] However, microcantilevers lack the inherent ability to selectively identify chemicals of interest. The key to overcoming this challenge is to functionalize the top surface of the microcantilever with a sorbent layer (i.e., polymer) that allows for selective binding between the microbeam and analyte(s) of interest.

Molecular imprinting involves arranging polymerizable functional monomers around a template, followed by polymerization and template removal.[3] This process is illustrated in Figure 1. Arrangement is generally achieved by noncovalent or reversible covalent interactions. In both types of molecular imprinting, once the template is removed, three-dimensional cavities are generated within the final materials that are complementary to the template molecule in size, shape, and functionality. Essentially, one creates a molecular "memory" within the imprinted polymer matrix. This allows preparation of polymers which are selective for the adsorption of the target molecule of interest. Other advantages of this technique include: robustness and stability under a wide range of chemical and physical conditions, and an ability to easily design recognition sites for a plethora of target chemicals (e.g., pesticides, energetic materials, pharmaceuticals and proteins).[4, 5]

Chemical, Biological, Radiological, Nuclear, and Explosives (CBRNE) Sensing XVI,
edited by Augustus Way Fountain III, Proc. of SPIE Vol. 9455, 94550W · © 2015
SPIE · CCC code: 0277-786X/15/$18 · doi: 10.1117/12.2179694

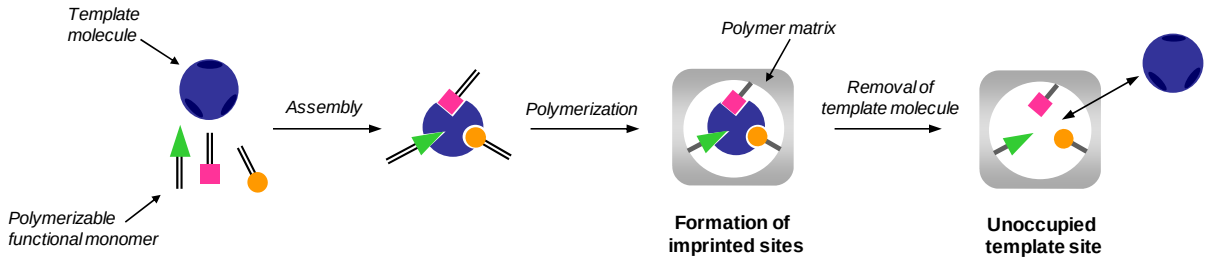

Figure 1. Simplified schematic of MIP fabrication.

In the current work, the polymer materials of interest are sol-gel-derived xerogels, which have been used as a platform for MIP-based sensor development.[6-8] These materials are attractive because their physicochemical properties can be adjusted by choice of precursor(s) and the processing protocol.[9] Precursors were chosen based on potential interactions with the explosive 2,4,6-trinitrotoluene (TNT). These specific interactions allow for increased target recognition. For example, MIPs comprised of 3-aminopropyltriethoxysilane (APTES) have been shown to engage in strong noncovalent interactions with TNT molecules via the formation of a charge-transfer complex between the electron-deficient aromatic ring of nitro-aromatics and the electron-rich amino group of the precursor.[10, 11] This interaction significantly improves polymer selectivity and affinity for TNT.[5] Similarly, hydrogen bond acidic precursors were chosen based on specific interactions with the chemical warfare agent (CWA) simulant dimethyl methyl phosphonate (DMMP) because they are strong sorbents for hydrogen bond basic vapor analytes and have been used in the sensing of basic organophosphorus vapors, such as those produced by DMMP.[12]

A MIP alone does not meet the requirements for a sensor without some form of a transducer to convert the analyte interaction into a measureable signal. There is evidence in the literature of a variety of gravimetrical detection techniques applied to convert a MIP into a "sensor".[13-15] In recent years, low mass, high frequency and low cost micro/nano sensors utilizing mass loading of microcantilevers have drawn increasing attention in the area of gravimetric sensing[1, 2], and MIPs have become an attractive thin film coating for many microelectromechanical systems (MEMS)-based sensors.[16, 17] In this work, molecularly imprinted xerogel thin films have demonstrated selectivity and stability in combination with a fixed-fixed beam MEMS cantilever.[18, 19] Traditionally, mass sensing using MEMS resonators has been achieved based on the natural frequency shift due to an increase in resonator mass; however, noise has set the limit of detection for linear sensing.[20] As an alternative to using changes in the natural frequency, nonlinear dynamics induced by parametric excitation have led to successful cantilever-based sensor designs.[19, 21-23] Under nonlinear operation, the sensor is driven parametrically at twice its natural resonant frequency.[24] This produces a bifurcation, which manifests as a sudden jump in the response amplitude. The critical location of the bifurcation mass tracking is recorded by repeatedly sweeping the frequency towards the critical point until a large change in amplitude occurs. The excitation frequency is then reset, and the process starts again.[25, 26] Bifurcation mass sensing has demonstrated better detection sensitivity in the presence of measurement noise when compared to linear sensing in air[27]; however, the long settling time and its high dependency on sweep rate to noise ratio[28, 29] make it less desirable. Much faster acquisition and a lower limit of detection were achieved with a noise squeezing method, where changes in phase noise were used as a precursor to the actual bifurcation event.[30, 31] A noise-squeezing controller is implemented using a high speed LabVIEW™ field programmable gated array (FPGA) to keep the device operating close to the edge of instability and inhibiting large amplitude changes (Figure 2). As a result, close to three orders of magnitude improvement in acquisition rate is achieved.

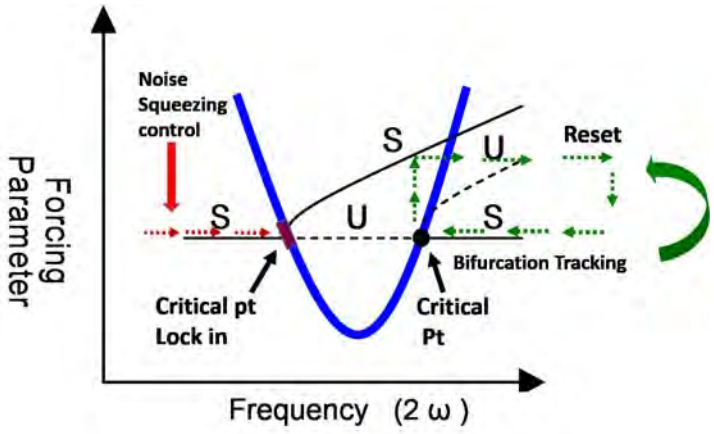

Figure 2. Schematic of both noise squeezing-based tracking (left) and bifurcation sweep-based tracking methods (right). The bifurcation sweep based tracking method tracks the bifurcation locations by repeatedly performing frequency sweeps towards a critical point until a large amplitude results. Then the device is relaxed to a zero stable state before the next sweep starts. In the noise squeezing control tracking method, the device approaches the critical point until the noise squeezes below some threshold, then feedback control keeps the device close to the edge of instability while maintaining a small response amplitude.

The goal of this research effort is to demonstrate that the MIP-coated microcantilever is an effective and robust chemical sensing scheme. The feasibility of the approach was assessed through polymer integration with fixed-fixed beam MEMS gas sensors using both noise-based and sweep-based bifurcation tracking, as well as the selectivity and stability of this sensor platform.

2. EXPERIMENTAL

2.1 Reagents and Materials

Aminopropyltriethoxysilane (APTES), methyltriethoxysilane (C1-TriEOS), 3-mercaptopropyl-trimethoxysilane (MPTMS), tetraethoxysilane (TEOS), and hydroxymethyltriethoxysilane (HMTriEOS) were obtained from Gelest. TNT was purchased from Cerilliant. DMMP, ethanol, and HCl were obtained from Sigma-Aldrich. All solvents were HPLC grade. All chemicals were used as received unless otherwise noted.

2.2 Device Fabrication

The sensors are fixed-fixed beams of varied lengths and widths. The beam thickness was 2 μm. The values were chosen so that the natural frequencies of the beams were less than half the natural frequency of the shear piezo actuator (330 kHz) used to drive the device. The microbeams were fabricated using a standard silicon on insulator (SOI) process [31]. The SOI wafer used was 2μm silicon (Si) device layer with 1 μm buried oxide and 520 μm Si handle. First, oxide was grown on both sides of the wafer. Silicon nitride (Si_3N_4) was deposited on the backside on top of silicon oxide; together they serve as masks to protect the backside for potassium hydroxide (KOH) etch in a later step. After front side oxide removal, it was then spun with photoresist and pattern was transferred. Then a deep reactive-ion etching was used to define the device features. Backside mask features were defined using photolithography and inductively coupled plasma. The front side was spun with a ProTEK® coating to protect features during backside release etch. The backside was opened by anisotropic KOH etch and stopped at the buried oxide. The device was then finished with removal of ProTEK and buried oxide layer.

2.3 Molecularly Imprinted Xerogels

Energetic MIP Preparation. A TNT stock solution was prepared at 9.85 x 10^{-3} M, in acetonitrile. Sol solutions were prepared by mixing C1-TriEOS (110 µL, 0.552 mmol), MPTMS (2.813 µL, 1.51 x 10^{-2} mmol), APTES (3.50 µL, 1.51 x

10^{-2} mmol), ethanol (1.25 mL, 21.4 mmol), and HCl (6.25 µL of 1M, 6.25 x 10^{-3} mmol). The C1-TriEOS, MPTMS, APTES, and HCl were added to the ethanol at room temperature and then stirred for 30 min to ensure a visually homogeneous sol solution. The TNT-doped sol solution was prepared by adding 150 µL of the TNT stock solution to the prehydrolyzed C1-TriEOS/MPTMS/APTES/HCl/ethanol sol solution. This sol solution was then vigorously mixed for 30 s with a touch mixer (Scientific Industries, Vortex-Genie 2). Xerogel thin films were formed by spin casting (4000 rpm, 2 min) a 50 µL aliquot of the final sol mixture onto a MEMS device using a spin coater (Laurell Technologies, model WS-400B-6NPP/LITE). The films were aged in the dark at room temperature for 2-3 days. TNT was extracted from the xerogel thin films with an ethanol/acetonitrile/acetic acid (v/v/v 8:2:1) solution. The xerogels were allowed to react with this solution at room temperature for 24 h. All xerogel thin films were subsequently rinsed with ethanol to remove the residual acidic solvent.

CWA MIP Preparation. Two different sol solutions were prepared. Solution #1 was prepared by mixing TEOS (1.26 mL, 5.64 mmol), deionized distilled (d/d) H_2O (205 µL, 11.4 mmol), ethanol (0.655 mL, 11.2 mmol), and HCl (5.62 µL of 0.1 M, 5.62 x 10^{-4} mmol). The TEOS, d/d H_2O, and HCl were added to the ethanol at room temperature and then sonicated for 1 h to ensure a visually homogeneous sol solution. The DMMP-doped sol solution was prepared by adding 75 µL of DMMP to the prehydrolyzed TEOS/H_2O/HCL/ethanol sol solution. This sol solution was then vigorously mixed for 30 s with a touch mixer. Solution #2 was prepared by mixing TEOS (250 µL, 1.12 mmol), HMTriEOS (250 µL, 1.11 mmol), d/d H_2O (7.5 µL, 0.416 mmol), ethanol (250 µL, 4.28 mmol), and HCl (1 µL of 0.1 M, 1 x 10^{-4} mmol). The TEOS, HMTriEOS, d/d H_2O, and HCl were added to the ethanol at room temperature and then stirred for 1 h to ensure a visually homogeneous sol solution. The DMMP-doped sol solution was prepared by adding 25 µL of DMMP to the prehydrolyzed TEOS/HMTriEOS/H_2O/HCL/ethanol sol solution. This sol solution was then vigorously mixed for 30 s with a touch mixer. For solutions #1 and #2, xerogel thin films were formed by spin casting (4000 rpm, 2 min) a 50 µL aliquot of the final sol mixture onto a MEMS device using a spin coater. The films were aged in the dark at room temperature for 2-3 days. DMMP was extracted from the xerogel thin films with H_2O. The xerogels were allowed to react with H_2O at room temperature for 5 h.

2.4 Control Xerogels

Control xerogel thin films were prepared by following the exact reaction sequences described above except TNT and DMMP were eliminated.

2.5 Sample Generation

The trace gases were generated using a calibration gas generator (VICI Metronics, model: Dynacalibrator 190). The energetic gas (2,4-dinitrotoluene (DNT)) source was two certified permeation tubes (KIN-TEK, model: HRT-007.50-2068/100) that were placed in the generator oven held at a constant temperature of 100 ºC. The permeation rate for both tubes at this temperature was 383 ng/min. Although the MIPs were developed for the detection of TNT, the structurally similar compound 2,4-DNT was used for the mass sensing experiments. 2,4-DNT is a degradation product of the unstable TNT molecule, as well as a manufacturing impurity found in the explosive.[32] Therefore, the detection of 2,4-DNT would be beneficial in recognizing the presence of TNT in the field. The CWA gas (DMMP) source was a certified permeation tube (VICI Metronics, model: Dynacal 107-150-7845-C100, length: 15 cm) that was placed in the generator oven held at a constant temperature of 100 ºC. The permeation rate at this temperature was 1180 ng/min. Nitrogen (N_2) was used as the carrier gas. The flow rates were controlled by mass flow controllers (MFC). The concentration of the analyte/N_2 mixture in parts per billion (ppb) can be calculated based on the flow rate and oven temperature for a specific permeation tube.

2.6 Sensor Operation

The device under testing is comprised of a fixed-fixed microbeam, as shown Figure 3. The sensing experiments are conducted in a closed chamber at atmospheric pressure and room temperature. Figure 4 depicts the basic elements required for gas sensing using the microbeam. The sensor was mounted on a shear piezo, driven by a function generator

(Agilent, model: 33512B) at nearly twice the resonant frequency (to drive parametric resonance) at a fixed voltage of 32 V. The sensor response is detected by an optical laser Doppler vibrometer (LDV) (Polytec, model: OFV 511) and the signal is analyzed using a lock-in amplifier (Stanford Research Systems, model: SR830 DSP). The lock-in amplifier provides outputs that include the "in phase" component of the signal, $V_{sig}\cos\varphi$ (X) and the "quadrature" component, $V_{sig}\sin\varphi$ (Y). Amplitude and phase information of the signal can be calculated from the X and Y components. Based on the statistics of the phase, the FPGA controller (National Instruments, model: cRIO-9014 Compact Real-Time Control Board) provides feedback to the function generator to perform corresponding frequency modulation to remain at the edge of bifurcation instability.

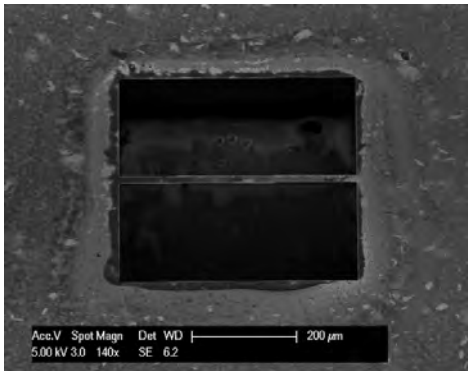

Figure 3. SEM image of a silicon fixed-fixed microbeam sensor coated with a MIP.

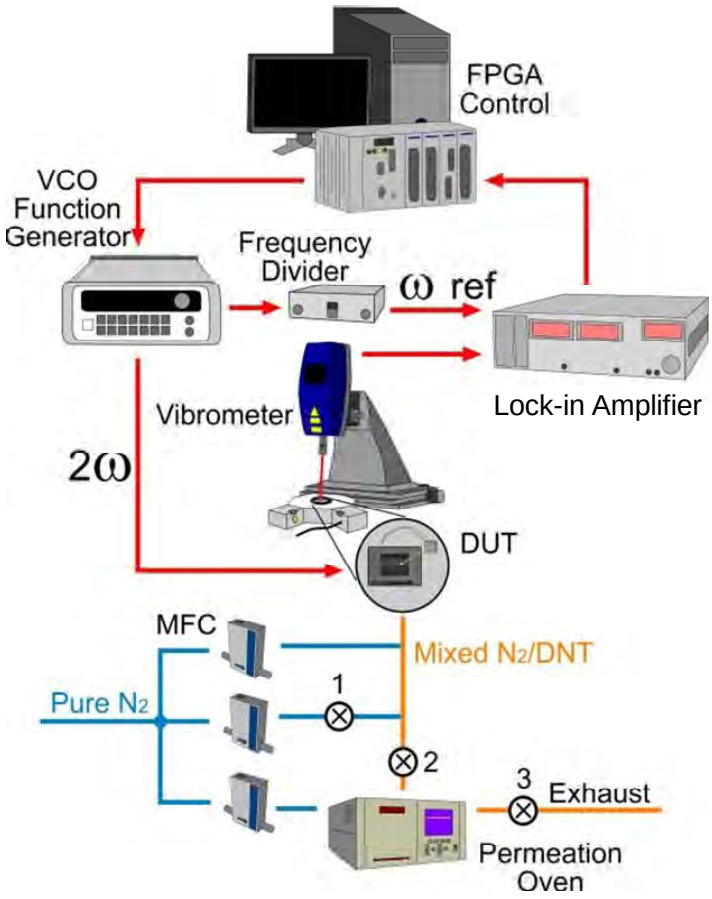

Figure 4. Simplified diagram of the experimental setup for gas sensing.

3. RESULTS AND DISCUSSION

There are several key challenges to overcome in the development of a MIP-coated microbeam MEMS sensing platform including: (1) developing a strategy for MIP integration to enable target interaction without compromising the frequency operation of the device; (2) developing a MIP formulation that is stable and integrated with the MEMS sensor to allow for practical application in the field; and (3) ensuring that the developed MIP allows for template removal, analyte reintroduction, and also provides selectivity for the target analyte components.

3.1 MIP Integration and Sensor Performance

MIP for Explosives Detection. The integrated MIP for explosives detection has shown that it is selective to 2,4-DNT and has demonstrated reliable reversibility and stability.[18] In this work, the gas sensing experiment was performed with the noise-squeezing controller at a concentration of 0.93 parts-per-billion (ppb) 2,4-DNT. Figure 5 presents the change in the natural frequency of the microbeam sensor over time as it is challenged with 2,4-DNT. A single response cycle included 15 minutes of pure N_2 followed by 10 minutes of 2,4-DNT. The sensor was reset (i.e., the absorbed 2,4-DNT molecules released from the polymer matrix) using pure N_2 (purge). It is clear from Figure 5 that the polymer coating does not compromise the frequency operation of the device. The response is reversible after 9 cycles. During gas sensing experiments, switching from 2,4-DNT to pure N_2 by manually turning the corresponding valves caused the frequency to drop sharply before returning to an upward trend (see example circled in Figure 5). This was observed in both the noise-based and sweep-based bifurcation sensing strategies. This is not an artifact of the control. It is unique to the analyte sensing, as it is not visible in a similar experiment using water vapor (data not shown). One possible

explanation is that the release of 2,4-DNT molecules from the polymer uses so much energy that the beam is cooled and its natural frequency lowered for a brief moment, until it returns to room temperature.[33]

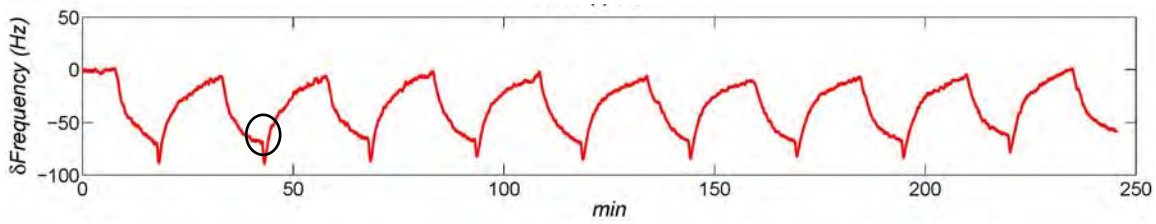

Figure 5. Natural frequency versus time plot for a typical MIP-coated microbeam sensor when it is challenged by 0.93 ppb 2,4-DNT and reset with N_2. The response is reversible after 9 cycles. The linear frequency drift of 0.05 Hz/min was accounted for in the post processing.

Further experiments were conducted at higher concentrations of 2,4-DNT. These experiments were carried out by the noise squeezing bifurcation sensing method (Figure 6) and the bifurcation sweep tracking method previously described[19] (Figure 7) for comparison. Figures 6 and 7 present sensor response data as a function of 2,4-DNT concentration. An increasing concentration of the analyte was introduced after the steady state of the previous (lower) concentration of analyte was reached. Hence, after each concentration of 2,4-DNT was introduced, no pure N_2 was used to release the absorbed 2,4-DNT molecules. The motivation for this test came from the observation that the coatings would not fully recover following an N_2 purge. It was therefore necessary to understand potential saturation effects. Each 2,4-DNT concentration increase resulted in a larger shift of natural frequency at saturation state in reference to the initial state (i.e., before introduction of 2,4-DNT). Therefore, this experiment was valid in finding the absorption calibration curve for the sensor.

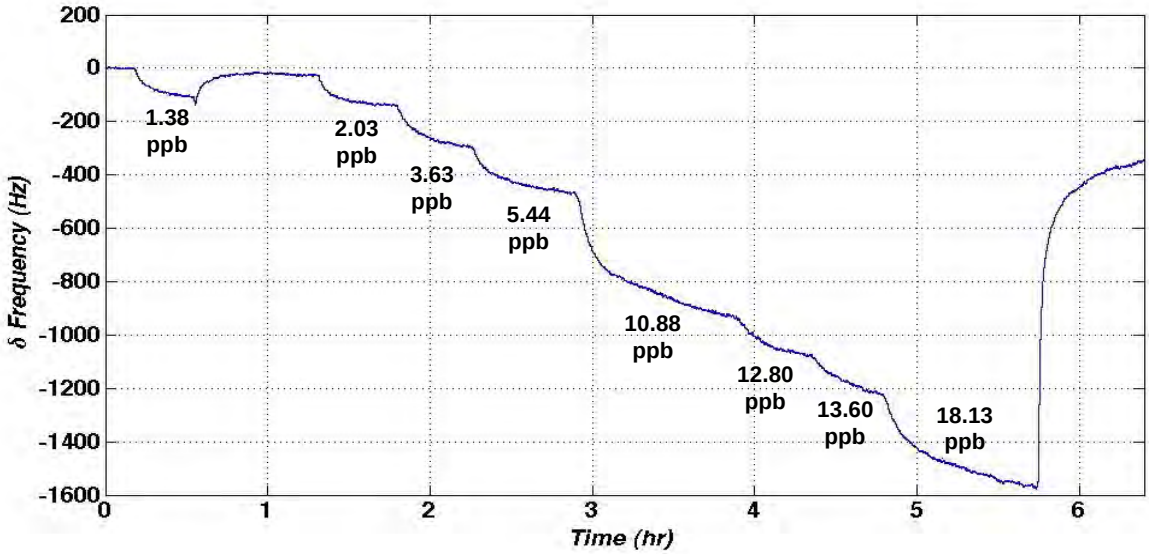

Figure 6. Data collected using the noise squeezing bifurcation tracking method. Natural frequency versus time plot for a typical MIP-coated microbeam sensor when it is challenged with increasing concentrations of 2,4-DNT. Absorbed 2,4-DNT was not completely purged from the sensor using pure N_2 after the first cycle (i.e., 1.38 ppb 2,4-DNT), therefore the frequency did not return to the initial frequency.

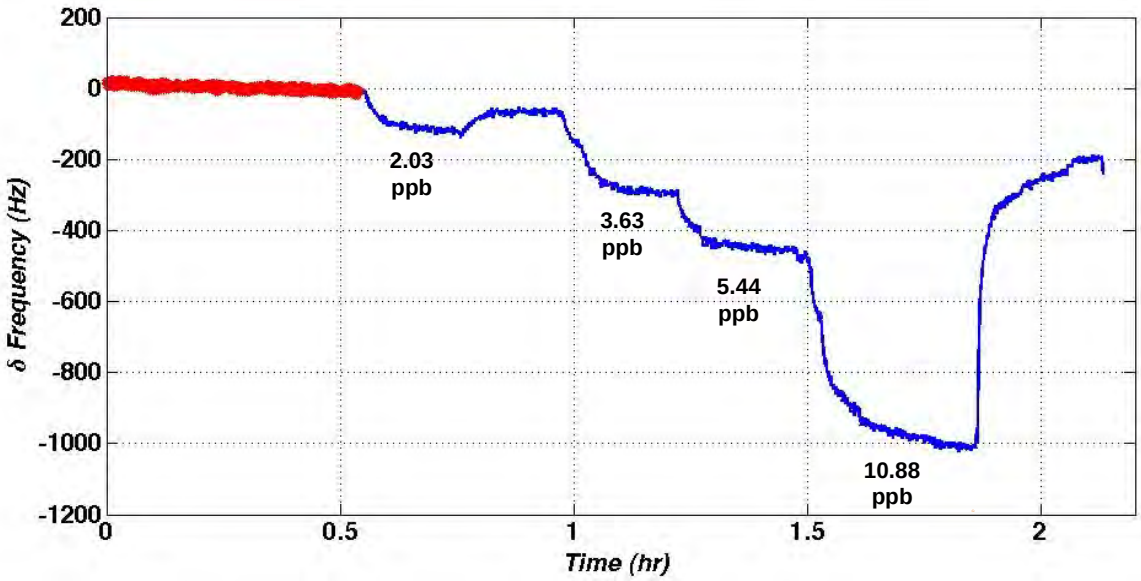

Figure 7. Data collected using the bifurcation sweep tracking method. Natural frequency versus time plot for a typical MIP-coated microbeam sensor when it is challenged with increasing concentrations of 2,4-DNT. Absorbed 2,4-DNT was not completely purged from the sensor using pure N_2 after the first cycle (i.e., 2.03 ppb 2,4-DNT), therefore the frequency did not return to the initial frequency.

The response profiles from a 2,4-DNT-responsive MIP-coated microbeam MEMS sensor to increasing concentrations of 2,4-DNT are illustrated in Figure 8. Data from both the noise squeezing bifurcation tracking and the bifurcation sweep tracking methods is shown. For both methods, the frequency shift increases as the 2,4-DNT concentration increases and the results exhibit excellent linearity. Coefficients of determination (R^2) can be found in Figure 8. Specific limit of detection (LOD) values are also provided in Figure 8. It is important to note that the frequency shift shown in all figures in this work (for 2,4-DNT detection) corresponds to the drive frequency shift. Therefore, to relate them to the natural frequency shift, a multiplication factor of 0.5 is needed. The Allan deviation[34] was used to quantify the frequency stability of the background signal (i.e, the minimum frequency that can be detected). The LOD was calculated by taking the minimum frequency and dividing it by the slope of the linear function.

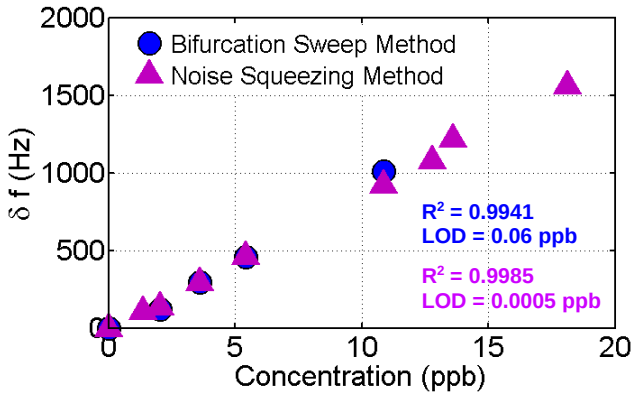

Figure 8. Response profiles from a 2,4-DNT-responsive MIP-coated microbeam MEMS sensor to increasing concentrations of 2,4-DNT using both the noise squeezing method and bifurcation sweep tracking method. Note that the frequency shift in this figure corresponds to the drive frequency, so the actual natural frequency shift is half of what is indicated. Error bars are negligible.

Experimental results demonstrate that noise-squeezing control for bifurcation sensing is a better sensing strategy than the bifurcation sweep method previously described.[19] It uses the statistics of the phase noise as a precursor to the bifurcation event, and the control time is less than 10 ms. The average time for a bifurcation sweep method to track a bifurcation event is 15 to 20 seconds, depending on sweep rate. More than three orders of magnitude improvement in acquisition is achieved using the noise squeezing method for bifurcation detection. The advantage of the noise squeezing method is evident in the frequency stability of the sensor, which is over two orders of magnitude smaller than that of the bifurcation sweep method. This is significant because it means two orders improvement in ultimate sensitivity of the sensor. Furthermore, fast data acquisition employing the noise squeezing strategy not only results in higher confidence on the estimation of the bifurcation locations, but also enables more information on the response dynamics of the MIP. As a result, the noise squeezing-based bifurcation tracking can be used for other applications in addition to mass sensing, for example, to characterize the absorption kinetics of the MIP to further improve surface coating chemistry. It should be noted that the sensor sensitivity to the absorption of 2,4-DNT is directly correlated to the surface coating chemistry.

As expected, the response from a control-coated microbeam MEMS sensor when it was challenged by 2,4-DNT was inferior compared to the MIP-coated sensor. This data has been previously described using the bifurcation sweep tracking method.[19]

MIP for CWA Detection. The integrated MIP for CWA detection was designed based on specific hydrogen bonding interactions with DMMP and have been demonstrated for gas phase sensing of the organophosphorus vapors produced by this analyte.[12] In this work, the gas sensing experiment (i.e., sensor response cycles over a period of time at a single DMMP concentration) was performed with the noise-squeezing controller (data not shown). The following results are for a MIP coating derived from sol solution #1. MIP-coated cantilevers for which the polymer coating was derived from sol solution #2 were not investigated due to an inability to get the cantilevers to bifurcation.

Further experiments were conducted at higher concentrations of DMMP. These experiments were carried out by the noise squeezing bifurcation sensing method. Figure 9 presents sensor response data as a function of DMMP concentration. An increasing concentration of the analyte was introduced after the steady state of the previous (lower) concentration of analyte was reached. Hence, after each concentration of DMMP was introduced, no pure N_2 was used to release the absorbed DMMP molecules. Each DMMP concentration increase resulted in a larger shift of natural frequency at saturation state in reference to the initial state (i.e., before introduction of DMMP). Therefore, this experiment was valid in finding the absorption calibration curve for the sensor.

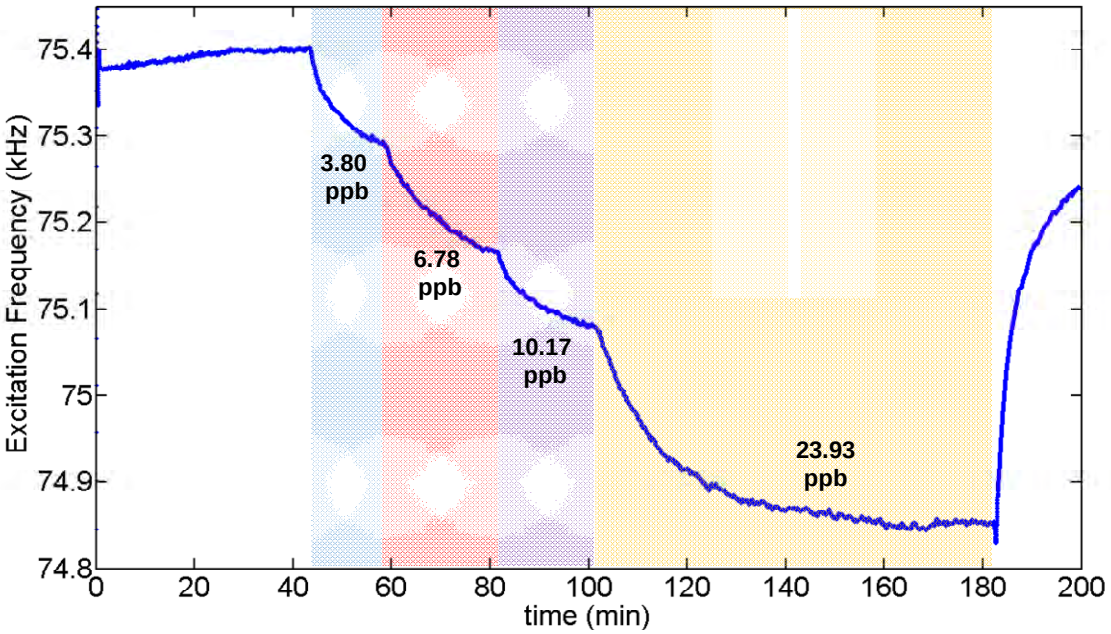

Figure 9. Data collected using the noise squeezing bifurcation tracking method. Excitation versus time plot for a typical MIP-coated microbeam sensor when it is challenged with increasing concentrations of DMMP. Absorbed DMMP was not completely purged from the sensor using pure N_2 after the first cycle (i.e., 3.80 ppb DMMP), therefore the frequency did not return to the initial frequency.

A similar set of experiments were conducted using a control-coated microbeam MEMS sensor. Figure 10 presents sensor response data as a function of DMMP concentration. Due to the presence of hydrogen bond acidic precursors in the control xerogel and the resulting strong sorbent functionality for organophosphorus vapor, it was expected that DMMP would react with this polymer.

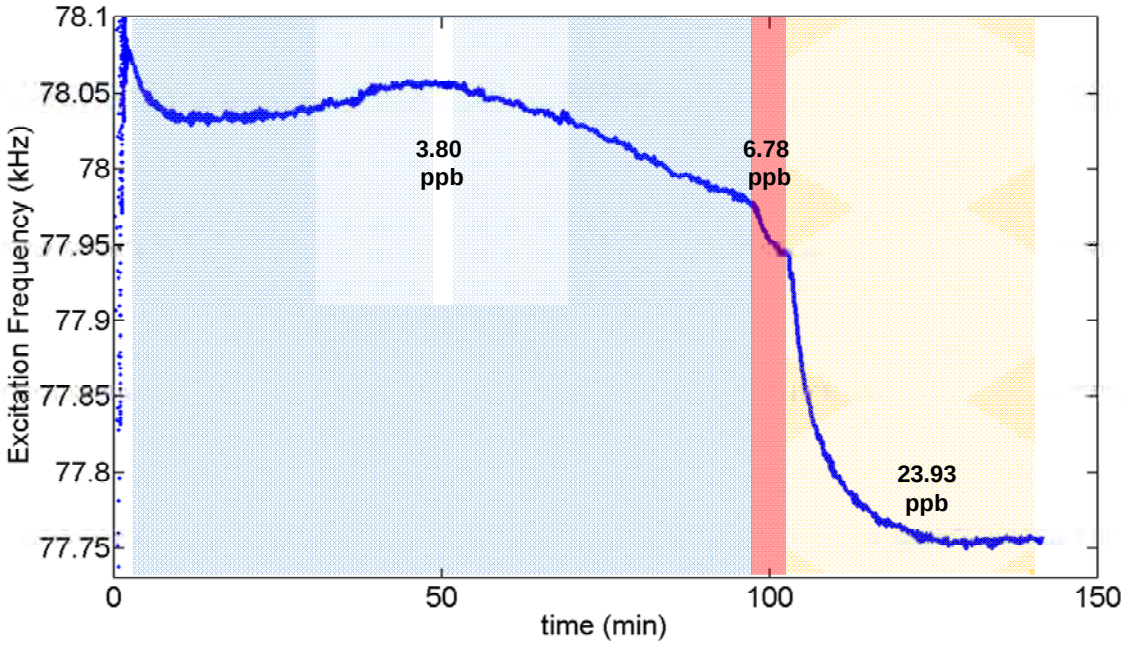

Figure 10. Data collected using the noise squeezing bifurcation tracking method. Excitation versus time plot for a typical control-coated microbeam sensor when it is challenged with increasing concentrations of DMMP. Absorbed DMMP was not completely purged from the sensor using pure N_2 after the first cycle (i.e., 3.80 ppb DMMP), therefore the frequency did not return to the initial frequency.

Figure 11 illustrates the microcantilever response profiles from DMMP-responsive and control xerogel coatings to increasing concentrations of DMMP. For the MIP-coated MEMS sensor, the frequency shift increases as the DMMP concentration increases. Binding properties were calculated using the Langmuir-Fruendlich (LF) isotherm, which is capable of modeling MIPs.[35] Non-specific binding is evident in the results from the blank (control) xerogel. These results demonstrate the selectivity and increased sensitivity of the MIP for DMMP. Coefficients of determination (R^2) can be found in Figure 11. Specific limit of detection (LOD) values are also provided in Figure 11. It is important to note that two different models were used to fit the response data for the energetic and CWA MIP-coated cantilevers. The polymer formulations and binding properties of each of these MIPs is very different, and therefore the response profiles were expected to vary as well.

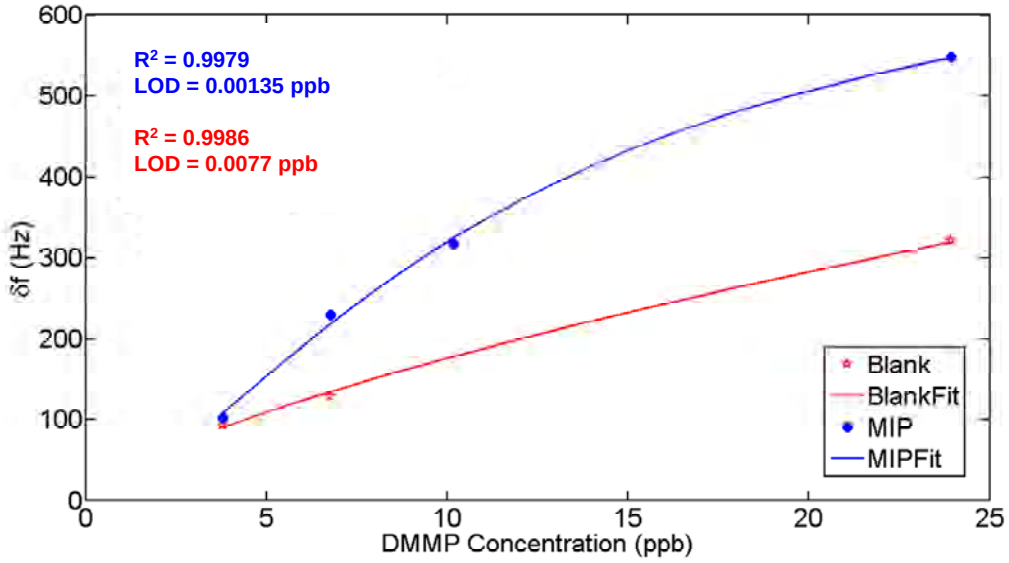

Figure 11. Response profiles from a DMMP-responsive MIP-coated and control coated microbeam MEMS sensor to increasing concentrations of DMMP using the noise squeezing method.

3.2 MIP Stability

In an effort to improve MIP adhesion to the MEMS device, the xerogel precursor, MPTMS, was included in the polymer formulation used to prepare the MIP for energetic recognition. The thiol group in this precursor chemisorbs onto a gold surface, which was applied to the microcantilever during device fabrication. This polymer showed excellent adhesion and stability, with no apparent degradation after 2 years, which is necessary for practical field use. Further testing is needed to determine the stability of the MIP for CWA recognition.

3.3 MIP Selectivity

To assess the selectivity of the MIP-coated microbeam MEMS sensors for 2,4-DNT and DMMP, the devices should be challenged by molecules that are structurally similar to the energetic and CWA analytes of interest. To demonstrate selectivity of the MIP for energetic detection, a MIP-coated microbeam sensor was challenged with toluene vapor. Toluene is the backbone molecule of both 2,4-DNT and TNT. This data has been previously described using the bifurcation sweep tracking method.[19] The selectivity of the MIP for CWA detection has not yet been assessed.

4. CONCLUSION AND FUTURE WORK

The work reported here validates the MIP-coated microcantilever sensing concept and demonstrates the feasibility of this MEMS sensor for the detection of explosive compounds and CWAs. To date, this is one of the only demonstrations of a MIP-coated microbeam MEMS sensing platform for these targets. Although preliminary, the data suggests that this combination is an effective and robust chemical nanosensing scheme. Further investigations will focus on refinement of the MIP (i.e., xerogel formulation) for improved selectivity. Finally, the MIP-coated microcantilever sensor platform evaluation should be expanded to include other explosives and chemical warfare agents of interest to the Army. A successful MIP-coated microbeam MEMS sensing format could reduce sensor cost and size, while maintaining the high sensitivity, selectivity, and portability needed for military applications.

5. REFERENCES

[1] H. P. Lang *et al.*, A chemical sensor based on micromechanical cantilever array for the identification of gases and vapors. Appl. Phys. A 66, 561 (1998).

[2] F. M. Battiston *et al.*, A chemical sensor based on a microfabricated cantilever array with simultaneous resonance-frequency and bending readout. Sens. Actuators, B 77, 122 (2001).

[3] M. Yan, O. Ramstrom, Eds., *Molecularly Imprinted Materials: Science and Technology*, (Marcel Dekker, New York, NY, 2005).

[4] E. L. Holthoff, F. V. Bright, Molecularly templated materials in chemical sensing. Anal. Chim. Acta 594, 147 (2007).

[5] N. R. Walker *et al.*, Selective detection of gas-phase TNT by integrated optical waveguide spectrometry using molecularly imprinted sol-gel sensing films. Anal. Chim. Acta 593, 82 (2007).

[6] A. L. Graham, C. A. Carlson, P. L. Edmiston, Development and characterization of molecularly imprinted sol-gel materials for the selected detection of DDT. Anal. Chem. 74, 458 (2002).

[7] M. K. P. Leung, C.-F. Chow, M. H. W. Lam, A sol-gel derived molecular imprinted luminescent PET sensing material for 2,4-dichlorophenoxyacetic acid. J. Mater. Chem. 11, 2985 (2001).

[8] E. L. Shughart, K. Ahsan, M. R. Detty, F. V. Bright, Site selectively templated and tagged xerogels for chemical sensors. Anal. Chem. 78, 3165 (2006).

[9] C. J. Brinker, G. W. Scherer, *Sol-Gel Science*. (Academic Press, New York, NY, 1989).

[10] A. Rose, Z. Zhu, C. F. Madigan, T. M. Swager, V. Bulovic, Sensitivity gains in chemosensing by lasing action in organic polymers. Nature 434, 876 (2005).

[11] C. Xie *et al.*, Molecular imprinting at walls of silica nanotubes for TNT recognition. Anal. Chem. 80, 437 (2008).

[12] I. Levitsky, S. G. Krivoshlykov, Rational design of a nile red/polymer composite film for fluorescence sensing of organophosphonate vapors using hydrogen bond acidic polymers. Anal. Chem. 73, 3441 (2001).

[13] F. Horemans *et al.*, MIP-based biomimetic sensor for the impedimetric detecion of histamine in different pH environments. Sens. Actuators, B 148, 392 (2010).

[14] R. Thoelen *et al.*, A MIP-based impedimetric sensor for the detection of low-MW molecules. Biosens. Bioelectron. 23, 913 (2008).

[15] D. Croux *et al.*, Development of multichannel quartz crystal microbalances for MIP-based biosensing. Phys. Status Solidi A 209, 892 (2012).

[16] C. Ayela, F. Vandevelde, D. Lagrange, K. Haupt, L. Nicu, Combining resonant piezoelectric micromembranes with molecularly imprinted polymers. Angew. Chem. Int. Ed. 46, 9271 (2007).

[17] J. A. Garcia-Calzon, M. E. Diaz-Garcia, Characterization of binding sites in molecularly imprinted polymers. Sens. Actuators, B 123, 1180 (2007).

[18] E. L. Holthoff, D. N. Stratis-Cullum, M. E. Hankus, A nanosensor for TNT detection based on molecularly imprinted polymers and surface enhanced Raman scattering. Sensors 11, 2700 (2011).

[19] K. L. Turner, C. B. Burgner, Z. Yie, E. L. Holthoff, paper presented at the 2012 IEEE Sensors, Taipei, Taiwan, 28-31 Oct 2012.

[20] K. L. Ekinci, Y. T. Yang, M. L. Roukes, Ultimate limits to inertial mass sensing based upon nanoelectromechanical systems. J. Appl. Phys. 95, 2682 (2004).

[21] V. Kumar *et al.*, paper presented at the ASME 2011 International Design Engineering Technical Conferences and Computers and Information in Engineering Conference, 2011.

[22] J. F. Rhoads *et al.*, Generalized parametric resonance in electrostatically actuated microelectromechanical oscillators. J. Sound Vibration 296, 797 (2006).

[23] M. Napoli, R. Baskaran, K. L. Turner, b. Bamieh, paper presented at the IEEE The Sixteenth Annual International Conference on Micro Electro Mechanical Systems, 2003, Kyoto, Japan, 23 Jan 2003.

[24] W. Zhang, K. L. Turner, Application of parametric resonance amplification in a single-crystal silicon micro-oscillator based mass sensor. Sens. Actuators, A 122, 23 (2005).

[25] N. Miller, C. B. Burgner, M. Dykman, S. W. Shaw, K. L. Turner, Fast estimation of bifurcation conditions using noisy response data. Proc. SPIE 7647, 76470O (2010).

[26] C. B. Burgner, N. Miller, S. W. Shaw, K. L. Turner, paper presented at the Solid-State Sensor, Actuator, and Microsystems Workshop, Hilton Head, SC, 2010.

[27] Z. Yie, M. A. Zielke, C. B. Burgner, K. L. Turner, Comparison of parametric and linear mass detection in the presence of detection noise. J. Micromech. Microeng. 21, 025027 (2011).
[28] M. Evstigneev, Statistics of forced thermally activated escape events out of a metastable state: most probable escape force and escape-force moments. Phys. Rev. E Stat. Nonlin. Soft Matter Phys. 78, (2008).
[29] P. Mandel, T. Erneux, The slow passage through a steady bifurcation: Delay and memory effects. J. Stat. Phys. 48, 1059 (1987).
[30] C. B. Burgner, K. L. Turner, N. Miller, S. W. Shaw, paper presented at the ASME 2011 International Design Engineering Technical Conferences and Computers and Information in Engineering Conference, 2011.
[31] L. L. Li, E. L. Holthoff, L. A. Shaw, C. B. Burgner, K. L. Turner, Noise squeezing controlled parametric bifurcation tracking of MIP-coated microbeam MEMS sensor for TNT explosive gas sensing`. J. MEMS 23, (2014).
[32] M. E. Walsh, T. F. Jenkins, P. G. Thorne, Laboratory and analytical methods for explosives residues in soil. J. Energ. Mater. 13, 357 (1995).
[33] T. Hiller, L. L. Li, E. L. Holthoff, B. Bamieh, K. L. Turner, System identification, design and implementation of amplitude feedback control on a nonlinear parametric MEM resonator for trace nerve agent sensing. J. MEMS early access online, (2015).
[34] D. W. Allan, Statistics of atomic frequency standards. Proc. IEEE Sensors 54, 221 (1966).
[35] I. Umpleby, R. J., S. C. Baxter, Y. Chen, R. N. Shah, K. D. Shimizu, Characterization of molecularly imprinted polymers with the Langmuir-Freundlich isotherm. Anal. Chem. 73, 4584 (2001).

1 DEFENSE TECH INFO CTR
(PDF) DTIC OCA

2 US ARMY RSRCH LAB
(PDF) IMAL HRA MAIL & RECORDS MGMT
TECHL LIB

1 GOVT PRNTG OFC
(PDF) A MALHOTRA

4 US ARMY RSRCH LAB
(PDF) ATTN RDRL SEE E
M FARRELL
E HOLTHOFF
P PELLEGRINO
G WOOD